

Nanoscale smoothing of plasmonic films and structures using gas cluster ion beam irradiation

Ee Jin Teo · Noriaki Toyoda · Chengyuan Yang ·
Andrew A. Bettiol · Jing Hua Teng

Received: 30 May 2014 / Accepted: 11 August 2014 / Published online: 24 August 2014
© Springer-Verlag Berlin Heidelberg 2014

Abstract We present a novel method of using gas cluster ion beam irradiation (GCIB) to flatten and widen grains in silver films and structures, while simultaneously, reducing the film thickness with nanometer precision. Ultrathin Ag films produced by GCIB have lower absorbance and better adhesion compared to as-deposited films. By applying the technique post-fabrication to plasmonic color filters, waveguides and disks, we show that an enhanced surface plasmon resonance and propagation length can be achieved.

1 Introduction

Using conventional thin film deposition techniques, such as electron beam evaporation, it is a challenge to produce ultrathin metallic films with low optical loss. The increase in optical loss with decreasing thickness is mainly attributed to the increase in scattering from grain boundaries and defects such as voids. This high loss limits many plasmonics applications that require ultrathin films such as the hyperlens [1] and superlens [2]. Long-range surface

plasmon polariton waveguides also utilize ultrathin metal films of <10 nm in thickness [3].

Previously, there have been several approaches employed with limited success for reducing scattering losses in thin metallic films, including depositing a seed layer [4] and thermal annealing. Although seed layer deposition can reduce surface roughness, it increases electron scattering through a reduction of grain size [5]. This often results in higher loss compared to the case when no seed layer is used. Thermal annealing can reduce scattering due to grain boundaries at the expense of an increase in surface roughness and a change in structure profile of the metallic nanostructure. Recently, we have employed a nanoprocessing technique using a gas cluster ion beam for producing ultrathin metallic structures with low loss [6].

GCIB was first developed by the Yamada's group in Kyoto University in 1992 [7]. It has since been used extensively for surface modification of optical, magnetic and semiconductor materials [8, 9]. It can also be used to enhance and promote cell proliferation in bioimplants [10]. A beam of N₂ gas cluster, consisting of thousands of molecules bounded by weak van der Waals forces, is first produced by supersonic expansion of the high pressure gas as it passes through a shaped nozzle into vacuum. The cluster is then ionized by electron bombardment and accelerated to 20 keV before it is directed onto the sample. Upon impact, the cluster disintegrates into individual constituent atoms with an average energy of a few eV. The sputtering effects of a cluster beam are vastly different from a monomer ion beam. Due to the high mass of each cluster and low energy/atom, a large energy density is delivered to a small volume with very low penetration depth. The target atoms are mostly ejected laterally from the impact site. This lateral sputtering process causes smoothing of irregularities on the surface, which is not

E. J. Teo (✉) · J. H. Teng
Institute of Materials Research and Engineering, 3 Research
Link, Singapore 117602, Singapore
e-mail: teoej@imre.a-star.edu.sg

N. Toyoda
Graduate School of Engineering, University of Hyogo,
2167 Shosha, Himeji, Hyogo 671-2280, Japan

C. Yang · A. A. Bettiol
Department of Physics, National University of Singapore,
2 Science Drive 3, Singapore 117542, Singapore

achievable with monomer ion beams. The individual atoms of a few eV are not energetic enough to cause subsurface damage normally associated with ion beam milling and plasma polishing process. Using the unique characteristic of GCIB bombardment, we have demonstrated the ability to reduce surface roughness of silver films and structures. We show how this technique can be suitably applied for plasmonic applications.

2 Experiments and results

First, electron beam evaporation is used to deposit a 70-nm thick Ag film onto a coverslip. Subsequently, GCIB irradiation was carried out using a 20-keV N_2 gas cluster ion beam with dose up to $2 \times 10^{16}/\text{cm}^2$. Atomic force microscope (AFM) of the surfaces was performed over a $1 \times 1 \mu\text{m}^2$ area before and after GCIB irradiation. Figure 1a shows a plot of the root mean square (RMS) roughness of the silver films with irradiation dose. For as-deposited Ag films, the surface exhibits a high level of faceting and surface roughness, caused by the polycrystalline growth. We see a high RMS roughness of $\sigma = 4.9$ nm. From the inset in Fig. 1a, we see a significant smoothing of the surface as the GCIB dose increase to $1 \times 10^{16}/\text{cm}^2$. The lateral sputtering caused by the low energy ions causes the crystallites to flatten and increase in lateral dimension. At a dose of $1 \times 10^{16}/\text{cm}^2$, σ is reduced to 1.50 nm.

During the smoothing of the surfaces, the GCIB process simultaneously sputters material from the metal layer. Figure 1b shows a plot of sputtered depth as a function of dose, with an initial starting thickness of 70 nm. We can see an increase in sputtered depth as doses increases to $2 \times 10^{16}/\text{cm}^2$. This shows the ability to control the sputtered depth to nanometer precision. From these measurements, it is possible to obtain Ag layers that are ultrathin (~ 15 nm) and smooth (~ 1.5 nm) at the same time. As the grains widen at the expense of flatter surface, lesser electron scattering is experienced from these ultrathin films, resulting in lower loss.

We have used this technique to produce ultrathin Ag films by sputtering to the desired thickness from a thicker layer. This is compared with as-deposited films of the same thickness. The thickness of the films is measured using AFM. We have measured the transmittance, reflectance and absorbance of the Ag films using a UV–Vis spectrophotometer. Figure 2 is the plot of the absorbance of the as-grown and GCIB processed Ag films at different thicknesses. From Fig. 2b, we can see an absorption peak appears at 450 nm for ~ 3 –4 nm Ag formed by GCIB. This is most likely due to the plasmon resonance absorption of nanoparticles or small clusters. As the metal thickness increases to 5.8 nm, the peak disappears and absorption

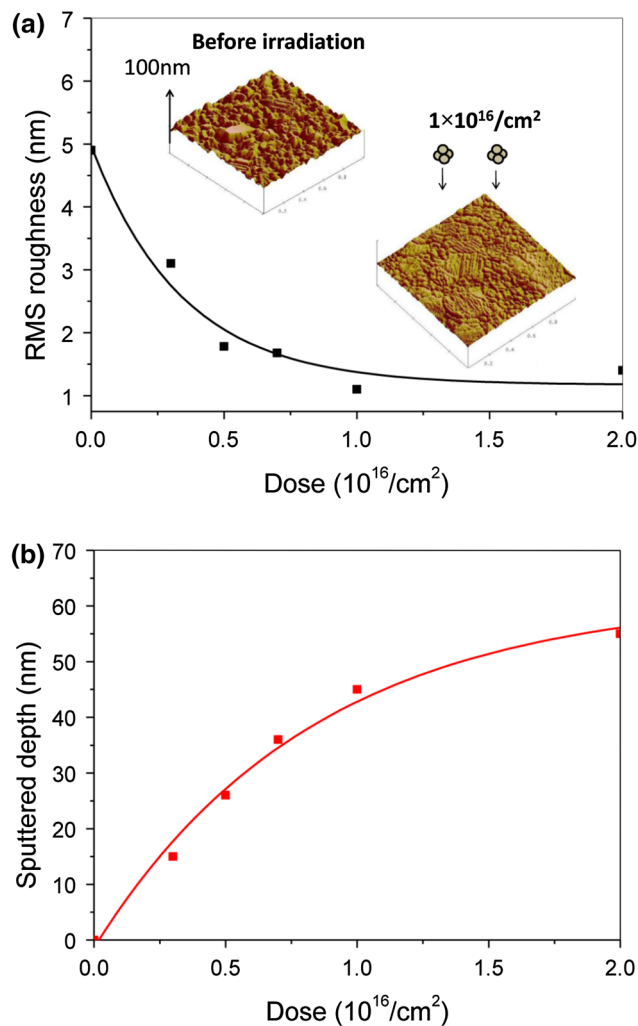


Fig. 1 Plot of **a** RMS roughness and **b** sputtered depth as a function of dose. *Inset* in (a) shows the AFM images of the Ag surfaces before and after irradiation

can be seen at longer wavelengths. Further increasing the thickness to 8.4 nm reduces the long wavelength absorption as the number of voids reduces. At 15 nm, the film is completely continuous and it becomes more reflective. On the other hand, the as-deposited films in Fig. 2a show much higher absorbance and a short wavelength peak can be seen for 12 nm and even 15 nm thickness. This disappears at a thickness of approximately 22 nm. From these measurements, we show that GCIB films have lower loss and percolation threshold. We can estimate the percolation threshold to be about 12 nm for as-deposited films and 3.5 nm for GCIB films.

3 Plasmonic color filters and disks

In this section, we have investigated the effect of GCIB irradiation on the localized surface plasmon resonance of

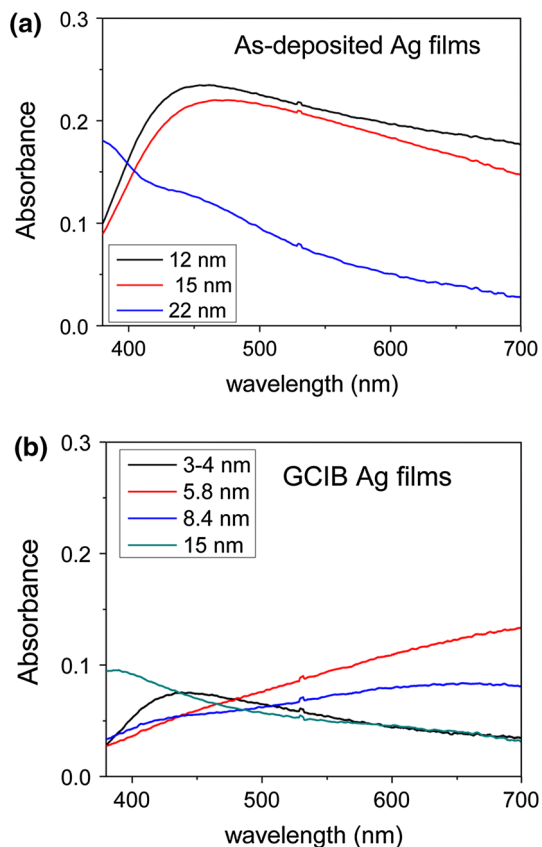


Fig. 2 Absorbance spectra for **a** as-deposited and **b** GCIB produced ultrathin Ag films

color filters. We have fabricated a series of color filters based on a square pillar array with a periodicity of 300, 200 and 120 nm and a thickness of 50 nm (Fig. 3a). Reflective color images are taken with optical microscope. It can be seen from Fig. 3b that the reflectance wavelength is shifted from red, to green to blue as the periodicity decreases from 300 to 200 nm and to 120 nm. Due to the thinning of the metal film thickness by the GCIB process, we have chosen a thicker starting layer of 70 nm so that we can compare the effect of GCIB on the resonance of the same thickness. We can see a slight improvement in the color purity. As the images are collected 1 month after fabrication, a reddish tinge can be seen on the perimeters of the green square, indicating a slight degradation of the resonance due to sulfidation. This disappears after GCIB irradiation and a more uniform color can be seen with stronger reflectance. This could be due to the smoother structures obtained after processing. It is also possible that GCIB may have removed the sulfidation layer and revived the plasmonic resonance of the color filters. More studies are needed to verify this point. According to our previous studies [6], we show that the structure profile is not affected or

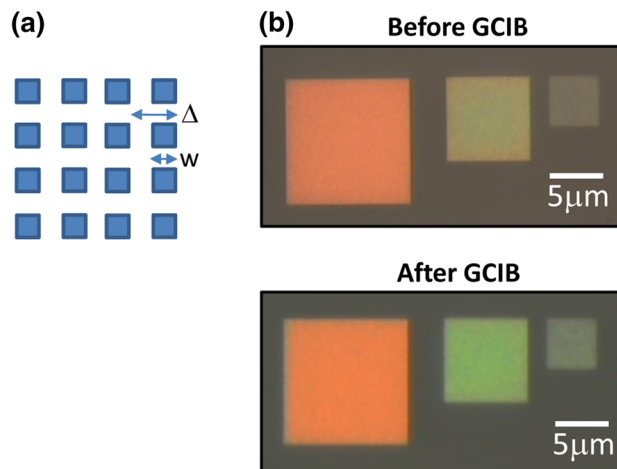


Fig. 3 **a** Square pillar array with a width and periodicity of ($w = 150$ nm, $\Delta = 300$ nm), ($w = 100$ nm, $\Delta = 200$ nm) and ($w = 60$ nm, $\Delta = 120$ nm) from *left to right*. **b** Reflectance images of the pillar arrays before and after GCIB treatment

modified by the irradiation. Due to the ultra-shallow penetration depth, only the first few nm of the silver layer has been amorphized, while the structural profile remains the same. This means that this technique can be used to process nanostructures compared to thermal annealing, which normally change the structure shape and profile.

The optical response of the fabricated nanosquare array was measured using a UV–Vis–NIR microspectrometer (CRAIC QDI 2010TM) at normal incidence with a 75-W broadband xenon source. We used an objective (magnification: 36 \times ; numerical aperture: 0.5) to illuminate white light onto the samples and collect the transmitted light into the spectrometer. The detecting area was limited to $5 \times 5 \mu\text{m}^2$ using a variable aperture. Transmission measurements were normalized with respect to a bare quartz substrate. It can be seen from Fig. 4 that the surface plasmon resonance has become sharper and deeper after GCIB treatment and the extra shoulder dip seen in the second and third spectra has disappeared (Table 1).

We have also studied the effect of GCIB on the surface plasmon propagation length of silver waveguides and disks using a WITec scanning near-field optical microscopy (SNOM) system. Light from a 632.8-nm He–Ne laser is focused onto the grating coupler through the substrate. Surface plasmons propagating in the metal waveguides are collected in the near field using a photomultiplier tube via a silicon tip with an aperture hole of 90 nm. By fitting the intensity profile along the waveguide to an exponential decay, we can determine the propagation length.

Figure 5 shows surface plasmon propagation in a (a) 5- μm -wide silver waveguide and a (b) 20- μm disk.

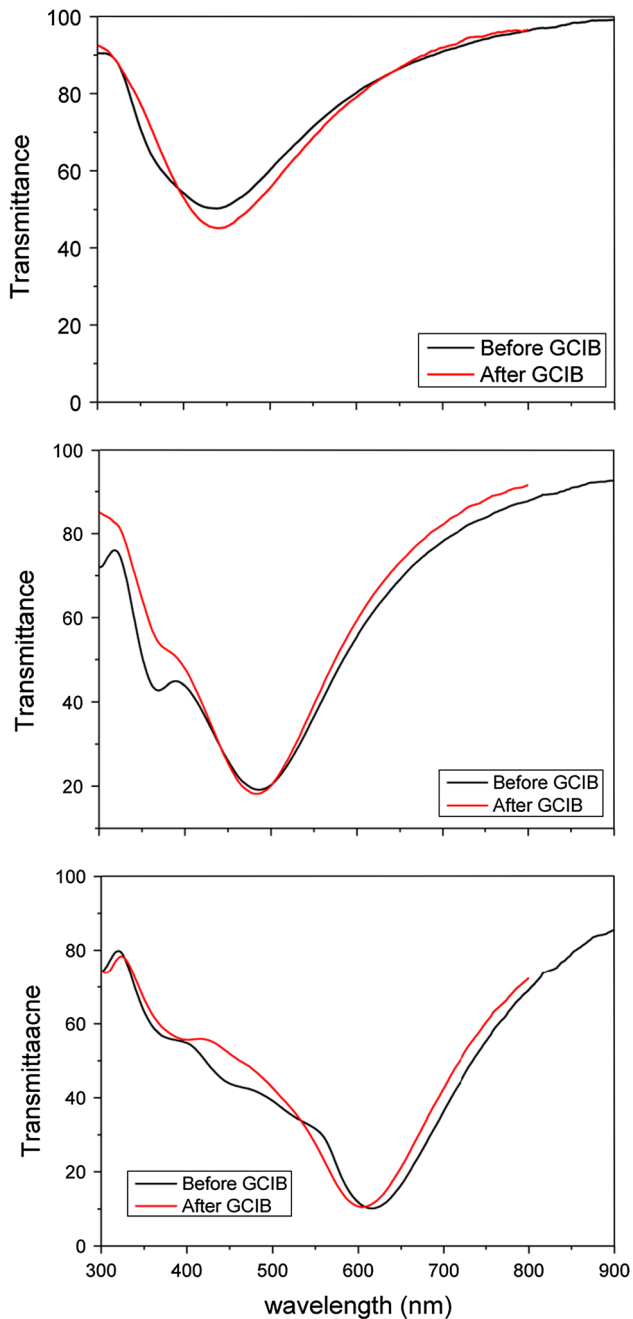


Fig. 4 Transmittance spectra for a square array with periodicity of 300, 200 and 120 nm (from top to bottom). The black and red curves indicate the spectra before and after GCIB treatment, respectively

Table 1 Showing the transmittance dip of color filters with different widths of the pillars, w , and periodicity, Δ

Transmittance dip (nm)	w , width (nm)	Δ , periodicity (nm)
441	150	300
487	100	200
610	60	120

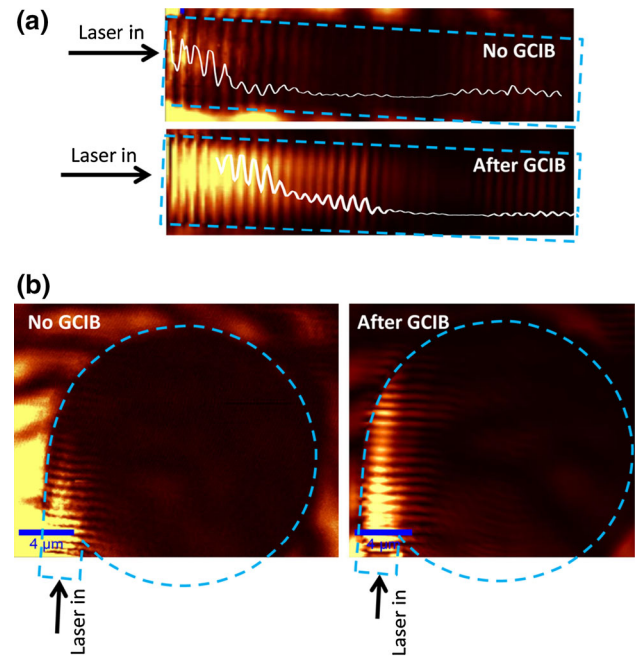


Fig. 5 SNOM images of **a** 5- μm -wide waveguides and **b** 20- μm -wide disk resonators before and after GCIB treatment. Dash blue lines indicate the outline of the waveguides and disks

Light is coupled into the optical devices via grating couplers. Due to etching by the GCIB process, the thickness of the structures reduces from 50 to 30 nm. We can see significantly longer propagation length after GCIB processing, as shown by the intensity profile in the waveguides. According to finite element method (FEM) simulations using Palik's data [11], the propagation length is about 7 μm before GCIB. The experimental result only yields a propagation length of 3 μm due to additional loss from scattering that was not considered in the simulations. On the other hand, good agreement between theoretical and experimental results is obtained after GCIB, indicating that damping loss is the main contribution to loss and scattering loss is minimized. From Fig. 5b, we can see a similar observation, whereby the GCIB processed disk shows a longer propagation length. However, one can see that the SP intensity is lost through the bends and through damping loss so that negligible propagation occurs inside the disk itself.

4 GCIB for adhesion promotion

Due to poor wettability and low bonding strength of Ag–O, it is difficult to obtain continuous thin films of noble metals on insulator. It also means that the adhesion of noble metal films and nanostructures to insulators is very poor. This poses a problem for fabricating nanostructures on

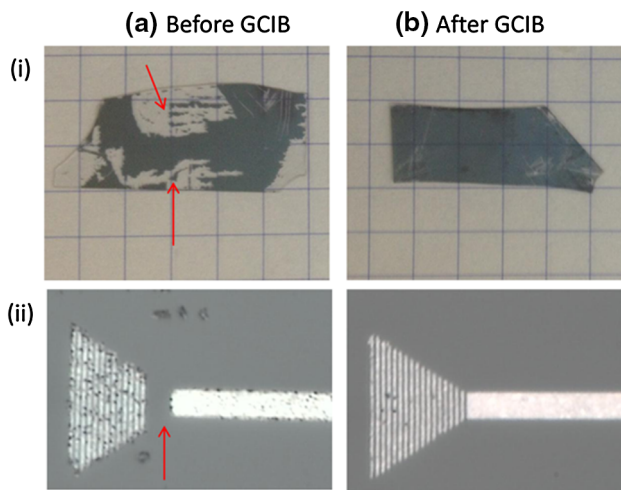


Fig. 6 Ag adhesion to coverslip **a** before and **b** after GCIB treatment using **i** Scotchtape test and **ii** prolong laser irradiation. The *red arrows* show the position of the laser spot on the gratings where light is coupled to the waveguide

insulators as the metallic nanostructures tend to lift off together with the photoresist rather than stay on the substrate during photoresist stripping in acetone. We show that GCIB can help improve the adhesion of metal films and nanostructures on coverslips (Fig. 6). We see that the Ag films and nanostructures can be peeled off easily with a scotch-tape or after prolong laser irradiation (in areas indicated by the red arrows). However, after subjecting to GCIB irradiation, the Ag films and nanostructures remain intact on the substrate, showing improved adhesion. From Fig. 6, we can also see that the waveguide suffers from sulfidation if left in air for about 1 month. This can be shown from the formation of pinholes at the edges of the waveguide and gratings. After applying the GCIB process, the waveguides are more resistant to degradation. This could be due to shallow nitrogen implantation in the Ag layer, acting as a protection layer against atmospheric degradation. Further investigations are needed to verify this point.

5 Conclusions

We show that GCIB is a new enabling technology for producing plasmonic films with improved optical absorbance and adhesion properties. It can also prolong the durability of the silver films which is important for plasmonic applications. By reducing the surface roughness and grain boundaries from the silver films and structures, we observed an enhanced plasmonic performance in plasmonic color filters, silver waveguides and disks. This development can bring plasmonic research a step closer to commercialization.

Acknowledgments This work was supported by A*STAR under Grant No. 0921540098, 0921540099 and 1223310075. E. J. Teo would also like to acknowledge the financial support from IMRE project code IMRE/12-1C0301 on plasmonic optical fiber sensor.

References

1. Y. Xiong, Z. Liu, C. Sun, X. Zhang, Two-dimensional Imaging by far-field superlens at visible wavelengths. *Nano. Lett.* **7**, 3360–3365 (2007)
2. J.B. Pendry, Negative refraction makes a perfect lens. *Phys. Rev. Lett.* **85**, 3966–3969 (2000)
3. I.D. Leon, P. Bernini, Amplification of long-range surface plasmons by a dipolar gain medium. *Nat. Photon.* **4**, 382–387 (2010)
4. V. Logeeswaran, N.P. Kobayashi, M.S. Islam, W. Wu, P. Chaturvedi, N.X. Fang, S.Y. Wang, R.S. Williams, *Nano. Lett.* **9**, 178–182 (2009)
5. W. Chen, K.P. Chen, M.D. Thoreson, A.V. Kildishev, V.M. Shalaev, *Appl. Phys. Lett.* **97**, 211107 (2010)
6. E.J. Teo, N. Toyoda, C.Y. Yang, B. Wang, N. Zhang, A.A. Bettiol, J.H. Teng, *Nanoscale* **6**, 3243–3249 (2014)
7. I. Yamada, *Radiat. Eff. Def. Solids* **124**, 69 (1992)
8. I. Yamada, N. Toyoda, *Nucl. Instrum. Meth. B* **241**, 589 (2005)
9. A. Kirkpatrick, *Nucl. Instrum. Meth. B* **206**, 830 (2003)
10. I. Yamada, J. Khoury, *MRS. Online Proc. Libr.* (2011), p. 1354
11. E.D. Palik, *Handbook of Optical Constants of Solids* (Academic Press, New York, 1991)